ESS LINAC BEAM PHYSICS DESIGN UPDATE

M. Eshraqi*, H. Danared, A. Jansson, Y. Levinsen, M. Lindroos, R. Miyamoto, M. Muñoz and A. Ponton, ESS, Lund, Sweden
R. De Prisco, ESS, Lund, Sweden and LNL-INFN, Legnaro, Italy

Abstract

The European Spallation Source, ESS, uses a linear accelerator to bombard the tungsten target with the high intensity protons beam for producing intense beams of neutrons. The nominal average beam power of the linac is 5 MW with a peak beam power at target of 125 MW. This paper focuses on the beam dynamics design of the ESS linac and the diagnostics elements used for the tuning of the lattice and matching between sections.

INTRODUCTION

The European Spallation Source, ESS-ERIC, is already under construction in the north of Lund, Sweden. The facility is financed with a single purpose of delivering highest flux of neutrons to users. Being a single purpose facility, the design parameters of the accelerator are defined by the high level requirements by neutron users and the design of neutron instruments at ESS. The high level parameters are the unprecedented power of 5 MW, a proton pulse of 2.86 ms and a repetition rate of 14 Hz. The ESS linac accelerates 62.5 mA of protons up to 2 GeV in a sequence of normal conducting and superconducting accelerating structures, these two parameters are defined through technology considerations and cost optimizations. The proton beam leaving the linac paints a rotating target where a high flux of neutrons is generated in the neutron rich target material at the same repetition rate.

Availability of the ESS facility is another one of the high level parameters. Having a high availability requires regular (and irregular) maintenance of the accelerator and the hands-on maintenance has set a limit of 1 W/m. In the ESS case a loss at such a level is in the order of 10^{-7} with respect to the total beam power, a very low density in the halo is tolerated.

LATTICE DESCRIPTION

Ion Source and LEBT A Microwave Discharge Ion Source is generating a proton pulse of up to 6 ms long with a flattop of up to~ 3 ms [1]. The proton intensity (H_1^+) exceeds 80 mA after the extraction electrodes at an energy of 75 keV. The MDIS has a high reliability of ~ 100% [2] and a long MTBF, very matched to the needs of a facility like ESS with high availability and reliability demands. The source is followed by the Low Energy Beam Transport, LEBT [3], which is composed of two magnetic solenoids (330 mm in length, 50 mm beam aperture radius and a maximum field of ~ 0.25 T). The LEBT matches the beam to the RFQ, has a chopper system removes low quality head and tail of the beam, a multi-blade iris to reduce the current and a suite of beam diagnostics that measure the beam. The gas pressure, distribution and composition in the LEBT is adjusted to compensate 95% of the space charge, this compensation is built within 20 μs when the proton beam passes through the LEBT. The ion source and LEBT are being designed and build by the INFN-LNS, Catania, Italy.

RFQ A four-vane RFQ is the first RF structure in the ESS linac; it accelerates, focuses and bunches the continuous 75 keV beam to 3.62 MeV [4, 5]. The RFQ length is chosen such that there is a good separation between quadrupolar and parasitic dipolar modes [6]; the final energy is optimized for improved acceleration in the RFQ plus the DTL system. The peak electric fields on the vane surface are limited to a Kilpatrick value of 1.9 at an rf frequency of 352.21 MHz. RFQ optical length is 4545 mm, with a minimum aperture of ~ 3 mm and a max. inter-vane voltage of 120 kV. The RFQ is being designed and built by the CEA Saclay, Saclay, France.

MEBT The Medium Energy Beam Transport system [7] measures, cleans and matches the beam out of the RFQ structure and transports it to the DTL. The MEBT is equipped with a suite of beam diagnostics to measure the current, transverse and longitudinal properties of the beam and provides means to collimate the beam in transverse using a 3 sets of 4 independently adjustable collimating blades [8]. The pulse has a head with 20 μs uncompensated space charge (and therefore mismatched), a fast stripline chopper device (with a repetition rate of up to 200 kHz) cleans this head and provides shorted pulsed needed for commissioning (in combination with the LEBT iris that creates lower current beams). The MEBT has 11 quadrupoles (80 mm magnetic length, 18.4 mm beam aperture, and ~ 2.6 T maximum integrated gradient) equipped with trajectory correcting coils (Maximum integrated field 2.8 mT.m) and 3 copper plated buncher cavities (14.5 mm beam aperture, maximum voltage of 150 kV and maximum power of 22.5 kW) resonating at the beam frequency. The MEBT is being designed and built by the ESS-Bilbao, Bilbao, Spain.

DTL The Drift Tube Linac accelerates the proton beam energy to 89.6 MeV in five tanks independently powered tanks [9–11]. Each tank is powered by a 2.8 MW klystron, reserving 30% margin for LLRF, tuning and waveguide losses, 2.2 MW of power is used to excite the cavity and accelerate the beam. At full beam current ~ 50% of this power is transferred to the beam and the rest is lost as ohmic loss. Higher energy at the DTL entrance results in longer low-energy cells with several positive consequences; longer cells could

* mamad.eshraqi@esss.se

ISBN 978-3-95450-147-2

house bigger quadrupoles reducing the magnetic gradient for the same integrated gradient, longer cells and gaps reduce the magnetic field and the electric field, respectively and higher energy enhances the effective shunt impedance, ZTT. The transverse focusing is provided by Halbach permanent magnet quadrupoles, PMQs (45 − 80 mm in length, beam aperture of 10−12 mm (Tank1-5) and a maximum integrated gradient of ∼ 3.1 T), that are housed in every other drift tube. The constraints present in a DTL requires an optimization process on where to put the corrector dipoles and BPMs and how to minimize the quantity. The DTL is being designed and built by the INFN-LNL, Legnaro, Italy.

Spoke Section The rest of the acceleration in the ESS linac is provided by superconducting cavities. A Low Energy Differential Pumping section, LEDP, separates the DTL from Spokes. Double spoke cavities [12] are used to accelerate the beam from 89.6 MeV to 216 MeV. The choice of spoke cavities is affected by the availability and reliability goals. These cavities can be retuned for different beam energies. Such a flexibility permits operation of the spoke section while a cavity [13] (or more) is nonoperational. Spoke cavities have a larger transverse aperture compared to conventional normal conducting structures. The 352.21 MHz spoke cavities (maximum gradient of 9 MV/m and beam aperture of 28 mm) with an optimum β of 0.50 are housed in pairs in 13 cryomodules [14] and are separated by Linac Warm Units, LWUs. Every LWU is composed of a pair of pulsed quadrupoles [15] (magnetic length 250 mm, beam aperture 30 mm, and maximum integrated gradient 1.9 T), a dual plane corrector (maximum integrated field 1.2 mT.m) and a BPM plus a central slot allocated to beam diagnostics. Depending on the required diagnostics per LWU there are different LWUs across the linac [16]. The spoke cavities and cryomodules are being designed and built by the IPN Orsay, Orsay, France, and all the corrector magnets and quadrupoles downstream of the DTL in Elettra, Trieste, Italy.

Elliptical Sections The RF frequency doubles to 704.42 MHz at the beginning of the next structure, the medium-β elliptical cavities. There are two families of elliptical cavities [17, 18] accelerating the beam from the spoke output energy to 571 MeV using 36 medium-β cavities (maximum gradient of 16.7 MV/m and beam aperture of 50 mm) and further to 2.0 GeV by 84 high-β cavities (maximum gradient 19.95 MV/m and beam aperture ∼ 68 mm). In both sections four cavities are housed in cryomodules of identical length [19, 20]. Having different geometric βs of 0.67 and 0.86 respectively, the medium-β cavities are given an extra cell (6-cell) with respect to high-β cavities (5-cell) to make the lengths of the two cavity types as close as possible. There are identical linac warm units, LWUs for both elliptical sections, before each cryomodule. Thus an equal the period length in the medium and high-β cryomodules, making them swap-able in case the required gradient in medium-β is not achieved. The elliptical LWUs have the same functionality as spoke LWUs, with stronger quadrupoles (maximum integrated gradient 2.3 T) bigger beam apertures (50 mm), and longer magnetic length (350 mm) plus stronger dual-plane magnetic correctors (integrated field 2.4 mT.m). To have the same flexibility at the spoke to medium-β transition the period lengths in elliptical section is chosen to be exactly twice that of the spoke section. The cryomodules are being designed and built in IPN Orsay, Orsay, France and CEA Saclay, Saclay, France, the medium-β cavities are designed in CEA Saclay and INFN-LASA, Milan, Italy, and the high-β cavities in CEA Saclay and Daresbury lab, Daresbury, UK.

HEBT The same periodicity, in transverse plane, is maintained for 15 periods after the high-β section in the High Energy Beam Transport, HEBT, for contingency purposes. After this contingency area, there is one more LWU which is followed by a vertical dipole with a bending angle of 4° that also works as a switch magnet between the beam dump and the target. In the path to target, after 6 periods of longer doublet focused sections that are adjusted to create an achromat dogleg, the beam is bent to horizontal plane using a second vertical dipole . This beam is transported to the target using a set of quadrupoles and 8 raster magnets that paint the target surface in horizontal and vertical directions at different frequencies [21]. To reduce the beam center movement on target due to energy jitter, the phase advance between the second dipole and the target surface is set to be a multiple of 180°. The raster magnets are being designed and built in Aarhus University, Aarhus, Denmark.

BEAM DYNAMICS

The ESS linac requires unprecedented loss control to stay below the 1 W/m of loss limit, and this sets a strong limit on the amount of halo produced in the linac. There has been several attempts to define the beam halo, e.g. [22, 23], and even more publications on the processes in which halo is generated, e.g. [24, 25]. One can summarize the most acknowledged sources of halo generation to mismatches, high space charge and tune depression, non-linear fields, and escape of particles from the accelerating bucket. The beam dynamics rules applied to the design of the ESS linac are:

- The zero current phase advance per period in all the planes must be less than 90°.
- The phase advance per meter (average phase advance) variation should be smooth and continues, at ESS on top of these the average phase advance changes also monotonically.
- The tune depression, $\eta = \sigma_{sc}/\sigma_0$, must stay above 0.4 in all the planes during acceleration, see Fig. 1.

Instead of choosing an equipartitioned beam, the SCL ESS linac is designed to have equal tune-depressions in the three planes [26], it was found out that an equipartition design would discriminate one (or more planes) in favor of

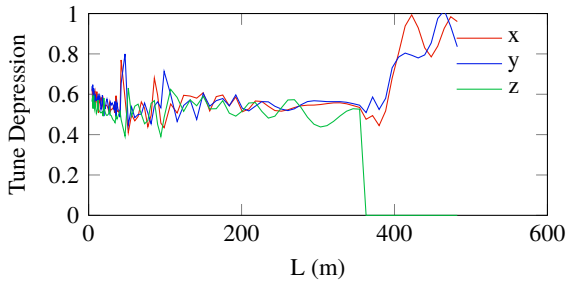

Figure 1: Tune depression in the ESS linac.

the other planes if the emittance ratios are not equal to 1, see Fig. 2. The codes TraceWin and Toutatis [27] are used

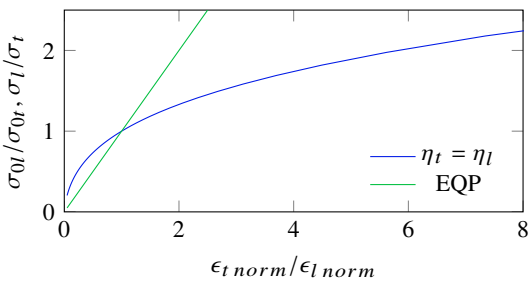

Figure 2: Values of $\sigma_{0l}/\sigma_{0t} = \sigma_l/\sigma_t$ for equal tune depressions (blue) and values of σ_l/σ_t for equipartition (green) as a function of the normalized emittance ratio.

to track the particles through the linac. Particle tracking for the simulations of the ESS linac is done in two steps, from the ion source exit (75 keV) to the end of RFQ. The output beam of RFQ is saved and used for the simulation of the rest of the linac. One million particles are tracked through the linac with 3D PIC space charge model and a 10^3 mesh.

To avoid particles escaping the accelerating bucket the synchronous phase is kept below $-15°$ at all times, with bigger values at lower energies, Fig. 3. Upstream of the

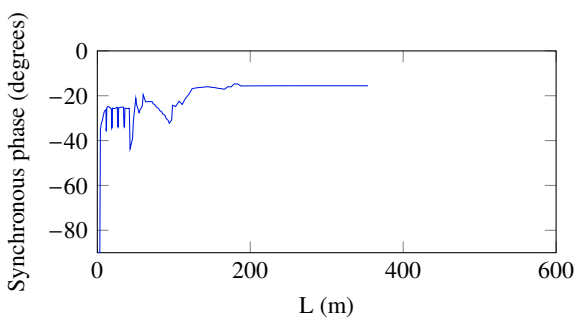

Figure 3: Synchronous phase in the ESS linac.

frequency jump the synchronous phases are gradually decreasing (towards more negative values) to keep the phase advance per meter equal to the phase advance per meter at the entrance of the next structure, medium-β section. Downstream of the frequency jump also the phases are bigger than what it would have been without the frequency jump, and the

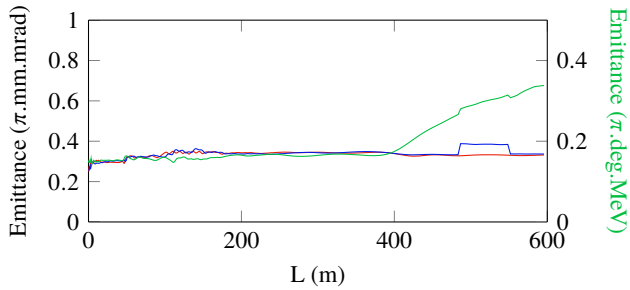

Figure 4: Emittance evolution in the ESS linac.

accelerating gradient is lowered to limit the phase advance per period to 90°. Having respected these design criteria the beam emittance for the machine without any errors does not dilute over the transport and acceleration, Fig. 4, and the halo parameter (proportional to the kurtosis of the distribution) stays almost constant, Fig. 5. The 99% emittances are also monitored to assure that the outlying particles does not behave differently, in transverse plane the ratio of 99% to rms emittance stays at ~ 12, and in longitudinal it increases to ~ 50 after the linac, where there is no more any external longitudinal focusing forces. The aperture to rms size ratio stays above 5 in the DTL, above 10 in spokes, and increases to beyond 20 at the beginning of high-β structure, permitting a low loss transport of beam even in the presence of errors [28].

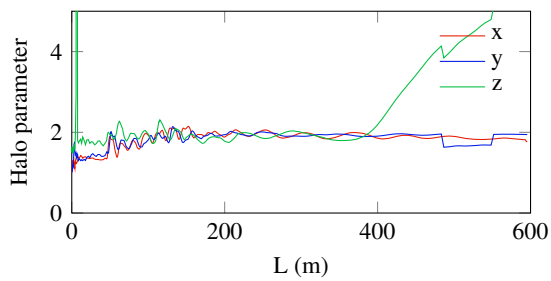

Figure 5: Halo parameter evolution in the ESS linac.

SUMMARY

The biggest beam dynamics challenges of the ESS linac are the requirements of very low halo production and low fractional losses of 10^{-7}. During the design and optimizations new models and beam physics theories have been developed at ESS, benefiting from these the current design, even though still improving, can deliver the requirements on losses and halo production given the tolerances on alignment, field quality and stability and diagnostics are achieved.

ACKNOWLEDGMENT

The ESS linac is being designed and build through a big collaboration with several European labs, institutes and universities. The authors would like to thank all the partners and contributors.

ISBN 978-3-95450-147-2

REFERENCES

[1] S. Gamino et al., "Preliminary Commissioning Results of the Proton Source for ESS at INFN-LNS", WEPMY035, IPAC 2016.

[2] L. Celona et al., Rev. Sci. Instrum. 75, 5 (2004).

[3] Y. I. Levinsen et al., "In-depth analysis and optimization of the European Spallation Source front-end lattice", TUPMR020, IPAC 2016.

[4] D. Chirpaz-Cerbat, "Status of the ESS RFQ", MOPOY054, IPAC 2016.

[5] A. Ponton, "Voltage Error Studies in the ESS RFQ", THPMB039, IPAC 2016.

[6] A. France, "Advanced RF Design and Tuning Methods of RFQ for High Intensity Proton Linacs", MOZA02, IPAC 2014.

[7] I. Bustinduy et al., "Current Status on ESS Medium Energy Beam Transport", TUO1AB04, HB 2014.

[8] R. Miyamoto et al.,"Beam Physics Design of the ESS Medium Energy Beam Transport", THPME043, IPAC 2014.

[9] P. Mereu et al., "ESS DTL1 Mechanical Design and Prototyping", WEPMB008, IPAC 2016.

[10] R. De Prisco, "ESS DTL Status: Redesign and Optimizations", THPME041, IPAC 2014.

[11] M. Comunian, "Progress on DTL Design for ESS", THPWO024, IPAC 2013.

[12] P. Duchesne et al., "Design of the 352 MHz, Beta 0.50, Double-Spoke Cavity for ESS", FRIOC01, SRF 2013.

[13] M. Eshraqi et al., "Preliminary Study of the Possible Failure Modes of the Components of the ESS Linac", ESS Tech. Note: ESS-doc-368-v3.

[14] D. Reynet et al., "Design of the ESS Spoke Cryomodule", MOP089, SRF 2013.

[15] D. Castronovo, R. Visintini, "On ESS LWU quadrupoles QC6 and QC7: DC and pulsed mode evaluation, magnet design and power supplies", ESS Technical Board Meeting, March 2015.

[16] A. Jansson, "Beam Diagnostics for ESS Commissioning and Early Operation", MOPMR20, IPAC 2016.

[17] P. Michelato, "ESS Medium and High Beta Cavity Prototypes", WEPMB011, IPAC 2016.

[18] E. Cenni et al., "Vertical Test Results on ESS Medium Beta Elliptical Cavity Prototype", WEPMB001, IPAC 2016.

[19] F. Peauger et al., "Progress in the Elliptical Cavities and Cryomodule Demonstrators for the ESS LINAC", TUPB007, SRF 2015.

[20] G. Olivier et al., "ESS Cryomodules for Elliptical Cavities" MOP084, SRF 2013.

[21] H. D. Thomsen, S. P. Møller, "Performance of the ESS High Energy Beam Transport under Non-nominal Conditions", WEPRO074, IPAC 2014.

[22] C. K. Allen, T. P. Wangler, "Beam halo definitions based upon moments of the particle distribution", PRST-AB, **5**, 124202 (2002).

[23] P. A. P. Nghiem et al., "Core-halo limit and internal dynamics of high intensity beams", Phys. Plasmas **22**, 083115 (2015).

[24] J. M. Lagniel, D. Libault, "Chaos, a source of Charge Redistribution and Halo Formation in Space-Charge Dominated Beams", PAC95, Chicago, 1995, p. 3235.

[25] J. Gao, "Analytical Estimates of Halo Current Loss Rates in Space Charge Dominated Beams", NIMA **484** 1-3, 2002.

[26] M. Eshraqi, J-M. Lagniel, "On the choice of linac parameters for minimal beam losses", IPAC 2013.

[27] D. Uriot, N Pichoff, "Status of TraceWin Code", MOPWA008, IPAC 2015.

[28] Y. I. Levinsen et al., "ESS 2015 Baseline Lattice Error Study", ESS Tech. Note: ESS-doc-377-v1.